# High Throughput Thermal Camera Characterization

**David Haefner and Stephen Burks**
US Army, Combat Capabilities Development Command (DEVCOM),
C5ISR Center, Research and Technology Integration Directorate
USA

david.p.haefner.civ@army.mil

## *ABSTRACT*

*Time and resource constraints often limit the number of cameras available to establish statistical confidence in determining if a device meets desired performance metrics. For thermal cameras, measurements of sampling/resolution, sensitivity and temporal response are typically specified by a user to ensure the device will be capable of performing the required tasks. Although many (not all) of these measurements are conducted by the manufacturer, often only a pass/fail will be reported along with notional/average values to some metrics. To gain insight into both individual as well as distributions of performance, it is desirable to conduct high volume testing. To accommodate a large volume of cameras, we utilized a rotation stage to iterate across the required measurements, with only a single connection instance to the camera. Automation in collection, processing, and device communication reduces opportunities for human error, further improving confidence in the results. Additional efficiency was accomplished through processing the measurements in parallel with data collection, reducing the time for full analysis of a single camera from approximately 30 minutes down to 4 minutes. From this work, a statistically relevant sampling of metrics was accumulated that allowed insight into manufacturing repeatability, correlated metrics, and dense datasets for device emulation. In support of the reproducible research effort, many of the analysis scripts used in this work are available for download at [1].*

## 1.0 INTRODUCTION

Camera procurement begins with describing what task(s) the camera is expected to perform. This typically involves defining a series of objects that should be observable under some specified environmental conditions (for example, distinguishing between a human and deer at night). The distance (range) of successful observation is the key parameter of interest, and what drives many design choices. The successful observation of an object requires both sufficient pixels across the object, and sufficient contrast of the object relative to the local background (and noise). This interplay between the number of resolvable pixels and the ratio of contrast to noise will depend both on the task and environmental conditions of operation. A useful image metric to evaluate the probability of task performance is the targeting task performance (TTP) metric [2]. The TTP metric utilizes many standard objective camera specifications combined through a nonlinear weighting (defined by the environmental conditions), and is commonly used in the original design validation and camera selection [3], [4].

The main objective parameters necessary for imaging tasks center on the resolution (resolved pixels on target) and the sensitivity (contrast-to-noise ratio). The resolution is decomposed into the angular sampling or instantaneous field of view (iFOV), which allows for the number of pixels on target to be evaluated. This is combined with the modulation transfer function (MTF), which specifies the amount of blur across the pixels on target. If the task involves any relative motion between the object and observer, the temporal response (thermal time constant, TTC, for a thermal camera) is also required to map temporal motion into an additional spatial blur. The contrast to noise ratio is found through the conversion factor (determined from the signal transfer function, SiTF) and the noise.

It is rare to measure all of the parameters necessary to predict range performance for each individual camera that goes to market. This is largely due to the time and resources necessary to complete such measurements. Instead, a small sampling of cameras is evaluated (usually during the design phase) and the variances between systems compared to expectations from the subcomponent tolerances and modeling. Modeling in this way typically assumes independence of the subcomponents, as the correlation between multiple parameters is often not available. To confirm the modeling, and to have confidence in compliance, full (repeatable) camera system level measurements should be conducted; and later compared back to the sub-component tolerance model. In this correspondence, automated methods to conduct complete camera measurements to allow for TTP metric range predictions are presented, enabling a full sampling of the correlated distributions of camera performance.

This paper is organized as follows: in Section 2, a review of the measurements used in calculating the TTP (sampling, blur, sensitivity, and time constant is given). In Section 3, the different time savings steps and automation methods are presented and compared to the standard sequence. In Section 4, the details of a thorough repeatability evaluation of the automated methods and analysis are presented. In Section 5, the automated and rapid methods are applied to a set of 250 cameras, demonstrating distributions. Finally, in Section 6, a review of the progress made in this work as well as plans for future improvements are discussed.

## 2.0 THERMAL CAMERA SPECIFICATIONS AND MEASUREMENTS

To ensure a camera will be successful for a specified task, without in situ evaluation, a model of task performance can be used (updated with measured camera parameters). The TTP metric is based on a linear systems approach to describing the imaging chain [2]; it combines information about the task parameters, environment, camera, display, and observer into a single number. The TTP metric utilizes residual image contrast through the atmosphere, camera, and display that the observer is capable of using to perform the task. In order to evaluate the TTP metric, a number of camera parameters are used to calculate the resolution and signal to noise [4]. In this section, we briefly review the measurement methods used to experimentally determine the camera parameters, specifically: sampling, blur, sensitivity (conversion factor and noise), and time constant.

### 2.1 Camera Measurements

The angular sampling (iFOV) of a camera determines the number of pixels across an object at a particular range. This is one of the most important metrics to determine successful task performance [3]-[6]. The iFOV is found as the ratio of the detector pitch (distance between pixels) to the focal length (assuming small angle approximation) and is typically specified for the center of the field-of-view. Experimentally, the iFOV can be determined through the use of a known angular sized target and measuring the number of pixels across it. It is important that the observed target is in focus such that the edge of the target can be determined accurately. For camera systems with a fixed focal position, the target should be placed at the correct range, or defocus should be accommodated in the edge location determination.

After the angular sampling has been determined, the next highest priority for performance prediction is the amount of blur, characterized through the MTF. As mentioned above, the MTF describes how the magnitude of spatial frequencies are modified by the camera. To measure an MTF, an input scene of known spatial frequency content is used, typically an edge or slit [7], [8]. Rotating the edge relative to the camera sampling enables one to resolve the edge spread function (ESF) at spatial frequencies beyond the Nyquist sampling limit. Following the capture of an image of an edge target, the region of interest (ROI) is selected. Care should be taken to ensure that the ROI is selected to provide sufficient size that the ESF has converged, but small enough that the blur from the opposite side is not impacting the ESF [9], [10]. The super-resolved ESF is found from projecting the 1 dimensional edge onto the axis orthogonal to the edge, utilizing the 2D sampling to provide additional samples. The line spread function, defined as the derivative of the ESF, is

found after applying a linear interpolation to the ESF. The magnitude of the discrete Fourier Transform is then calculated. The observed MTF is found after dividing the Magnitude of the discrete Fourier Transform by the transfer function associated with the discrete derivative, and then normalizing by the 0-frequency component .

Noise is the variations in a recorded signal while viewing a spatially and temporally constant target. For thermal cameras, this is measured experimentally from recording a video while viewing a blackbody source. The blackbody source typically subtends the entire FOV of the camera. In general, the noise from a thermal camera will exhibit variations in both space and time, which also exhibit some degree of correlation. A common method of describing the correlated noise is to decompose the 3D random process into the 7 independent components [11], [12]. These components span the permutations of 1D, 2D and 3D correlations to describe the full 3D cube and are commonly referred to as the 3D Noise model.

In order to estimate the SNR in device independent units, the noise in units of temperature [mK] is desired. This is accomplished through measuring the signal transfer function (SiTF). The SiTF describes how many counts are recorded by the camera for a given input temperature of a measured blackbody. The change in counts per unit temperature (Counts/mK) is then used to convert the noise into units of [mK]. Experimentally, this can be done by using as few as 2 measurements of known temperature; however a larger dynamic range and more samples provide additional context to the device response (for example linearity and saturation).

Although the temporal response for a thermal camera is not frequently measured, if a task involves any relative motion of the observer and the object of interest, the blur due to motion smear can quickly dominate the resolution. Measurement of the temporal response can be accomplished a number of ways, each involving inducing a temporal stimulus and recording a video. The method used in this work utilized imaging of a moving slit, where the motion created a spatial blur that could be fit to a parameterized model. Similar to the above resolution measurements, a collimator is used to ensure the slit is in focus for the system under test. A schematic of the experimental setup and the analysis sequence is shown below in Figure 1. The source behind the slit is a blackbody (45 [C]). The slit is closely aligned to the sampling of the FPA, and only a small vertical ROI is used. The small vertical ROI is critical for cameras with a rolling shutter read out, as each row will observe a delayed image of the moving slit.

To convert blur in pixels into blur in time, the pixels per second for the specific video is required. This can be calculated through knowledge of the linear velocity, iFOV, and focal length of the collimator. The pixels per second can likewise be found through fitting the pixels per frame to the data and knowing the frame rate of the video recording

$$PixPerSec = \frac{|LinVel|}{f_{col} \cdot iFOV} = FR \cdot |PixPerFrame| \tag{1}$$

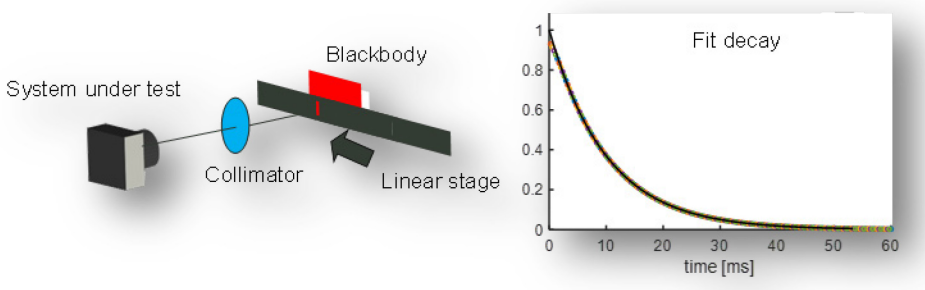


**Figure 1: (Left) Schematic of linear stage that moves a slit across the focus of a collimator, with a blackbody as the source behind it. (Right) the fit to the decay portion of the response.**

After the pixels per second and pixels per frame are found, the successive frames can be stacked on top of each other to provide a temporally oversampled intensity profile [4]. The typical model assumed for the temporal response of an uncooled camera is an exponential decay:

$$r_t(t) = \exp\left(-\frac{t}{\tau_{fit}}\right). \quad (2)$$

It is this function that is used to fit the decay portion of the super resolved slit video, show in Figure 1 (Right).

## 3.0 RAPID MEASUREMENT SEQUENCE

Measurements of thermal cameras must be done while the system is at equilibrium with the ambient environment (which should be carefully controlled from day to day). Depending on the system, this can take anywhere from a few minutes (for small systems) to hours (for large and unstable systems). Prior to measurement, the state of the camera should be adjusted to turn off scene-based processing. Once at equilibrium, the non-uniformity can be updated through a single point offset correction while flooding the full FOV with a blackbody at ambient. Following this, the blackbody is ramped to a pre-defined list of temperatures (in this case from 10 [C] in steps of 5 [C] up to 60 [C]), recording a video (128 [frames]) at each temperature.

Following the ramped blackbody capture, the next set of measurements conducted are the resolution measurements. To conduct these, the camera is moved from its position viewing the flooded field blackbody to looking down a collimator. Typically, 3 angular sampling measurements are conducted to reduce uncertainty in the reported iFOV. The MTF is measured in both the horizontal and vertical directions at the infinity projection.

Once the resolution measurement is completed, the thermal time constant measurements are conducted. Again, this will typically require an additional setup and moving the system under test. Once the camera has been moved, the capture must occur simultaneously while the slit is translated across the collimators focus. As mentioned above, for this study, 3 velocities in both directions were used to reduce uncertainty.

It is at this point that all the required data has been captured. Prior to turning the device off and repackaging the camera, it is useful to process the data and ensure accurate and uncorrupted measurements. Each of the above measurements requires a specified ROI, and it is expected that the engineer will select these accurately. Additionally, the information of one measurement will be applied to the following (for example, the analysis of the flat field SiTF data will provide an updated linear NUC and defective pixels to ensure the resolution and time constant measurements are accurate) therefore the analysis sequence must be done in a specific order. After all analysis has been completed, the modeled range performance is found and all the results are summarized in a report. The full measurement sequence is outlined below in Figure 2.

In order to facilitate a high volume of testing, the 22 [min] sequence in the previous section is insufficient. To begin refining the measurement sequence, the first issue addressed was to automate the communication with the device. This was chosen to optimize first as it reduced many potential areas of human errors. Through automated communication, the device serial number was retrieved and automatic file and folder naming created. While this only reduced the total time by 15 [s], it significantly reduces the stress on the engineer. The next time savings step taken was to automate the capture for both the resolution and time constant. This step did not significantly reduce the total time, an additional 2 [min] savings, but again reduced the strain on the test engineer and improves repeatability by reducing human error.

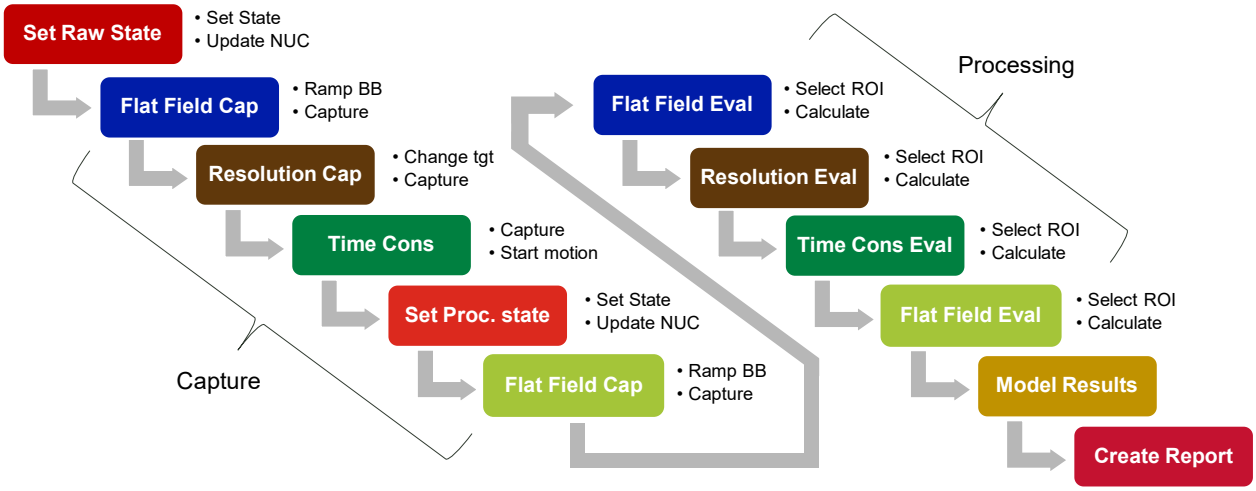


**Figure 2: Full measurement sequence from camera setup through range performance and report.**

The largest contributor to the total measurement time is the ramping and recording of the blackbodies. Each blackbody takes time to converge to the desired temperature. To obtain the same temperatures without waiting for convergence, 11 blackbodies set to the specified temperatures were used. To automate the capture, the camera system was mounted to a rotation stage and the blackbodies placed in a circle (See setup in Figure 3). At this point, the full sequence was reduced to less than 10 [min].

Further improvements in repeatability and expedited measurements could be accomplished through automating the region of interest and processing. To accomplish this, the regions of interest for an example systems were determined and registered to the measurement setup. From a 4 bar image of a system under test, the transformation between the new system under test and the measurement setup was established. This allowed for regions of interest to automatically be applied for each new system. Using the automated ROI, as well as automatic processing, further reduced the time by approximately 3 [min] down to around 7 [min] per system.

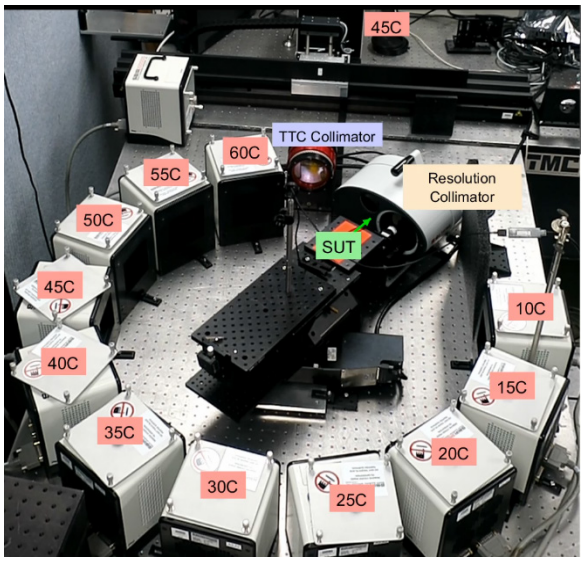


**Figure 3: The final configuration used for rapid and automated thermal measurements.**

The final optimization made was to use parallel methods in the analysis and capture. Immediately following capture, the analysis would be applied while the next measurement was being conducted. With this implemented, the total time to measure a camera was reduced to 4.3 [min], an approximately 18 [min] reduction. A full comparison of the decomposition of time saving methods is presented in the table below in Table 1.

**Table 1: Chart of the time saving methods used for rapid method.**

| | Manual | Auto Coms | Mount/Capture | Rotation stage | Auto ROI | Parallel |
|---|---|---|---|---|---|---|
| Set Raw State [s] | 30 | **10** | 10 | 10 | 10 | 10 |
| Flat Field Capture (11x) [s] | 330 (30) | 330 (30) | 330 (30) | **44 (4)** | 44 (4) | 44 (4) |
| Resolution Capture (6x) [s] | 150 (25) | 150 (25) | **60 (10)** | 60 (10) | 60 (10) | 60 (10) |
| Time Constant Capture (6x) [s] | 90 (15) | 15 | **30 (5)** | 30 (5) | 30 (5) | 30 (5) |
| Set Processing State [s] | 20 | **5** | 5 | 5 | 10 | 10 |
| Flat Field Capture (11x) [s] | 330 (30) | 330 (30) | 330 (30) | **44 (4)** | 44 (4) | 44 (4) |
| Flat Field Evaluation [s] | 50 | 50 | 50 | 50 | **40** | |
| Resolution Evaluation (6x) [s] | 120 (20) | 120 (20) | 120 (20) | 120 (20) | **60 (10)** | |
| Time Constant Evaluation (6x) [s] | 120 (20) | 120 (20) | 120 (20) | 120 (20) | **60 (10)** | |
| Flat Field Evaluation [s] | 50 | 50 | 50 | 50 | **40** | 40 |
| Model Results [s] | 20 | 20 | 20 | 20 | **10** | 10 |
| Create Report [s] | 20 | 20 | 20 | 20 | **10** | 10 |
| | | | | | | |
| Set State [min] | 0.83 | **0.25** | 0.25 | 0.25 | 0.33 | 0.33 |
| Capture Time [min] | 15.00 | 15.00 | **12.50** | **2.97** | 2.97 | 2.97 |
| Post Processing Time [min] | 5.67 | 5.67 | 5.67 | 5.67 | **3.33** | 0.67 |
| Summary Time [min] | 0.67 | 0.67 | 0.67 | 0.67 | **0.33** | 0.33 |
| Total Time [min | 22.17 | 21.58 | 19.08 | 9.55 | 6.97 | **4.30** |
| | | | | | | |
| Time Savings [min] | | 0.58 | 2.50 | **9.53** | 2.58 | 2.67 |

## 4.0 CAMERA MEASUREMENT REPEATABILTY ANALYSIS

Typically, measurements are defined by their accuracy and precision. The accuracy of a measurement refers to the errors of the average relative to the actual value. The actual value for a particular camera measurement is usually defined through the use of reference camera systems that have been calibrated across multiple measurement methods. With an automated measurement solution, statistics for the evaluation of repeatability can be conducted with very little user intervention. For this study, the same commercially available camera was measured 550 times across 4 days. Results of the repeatability for sensitivity measurements is shown below in Figure 4.

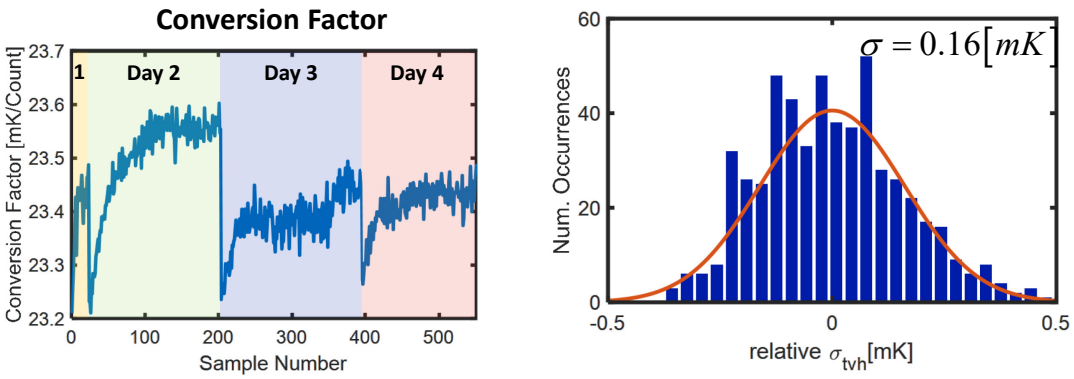


**Figure 4: (Left) Conversion factor across measurement days. (Right) the distribution of the noise.**

As can be seen, the conversion factor does exhibit some transient behavior with time for the different days. Additionally, the average value of the conversion factor on Day 2 appears to be higher than the other days. As the conversion factor for uncooled cameras is highly susceptible to the ambient conditions in the lab, correlations to ambient will be the subject of future studies. When this variation is combined with the repeatability of the noise measurements, the final uncertainty of the noise (in temperature units) was 0.16 [mK]. This value is expected to be significantly below the system to system variation for the camera systems to be tested. The distributions for the repeatability of the resolution and time constant are shown below in Figure 5.

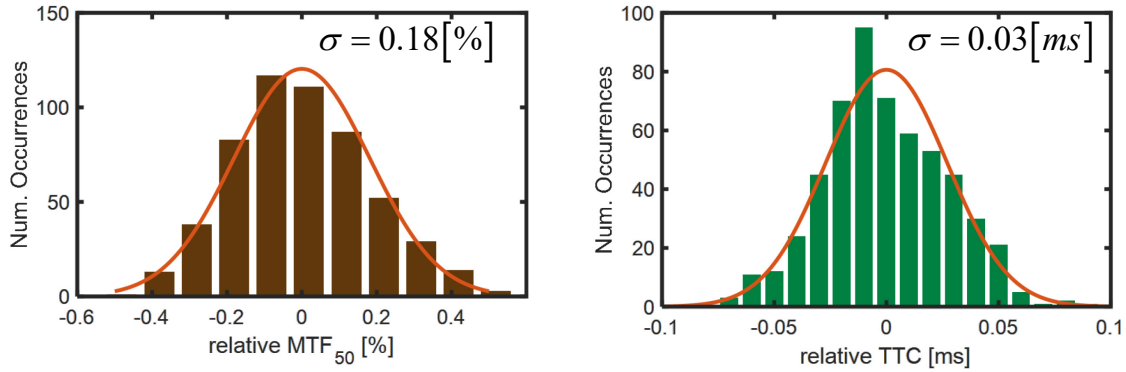


**Figure 5: (Left) Repeatability of resolution. (Right) Distribution of thermal time constant.**

## 5.0 MULTIPLE CAMERAS PARAMETER DISTRIBUTIONS

Following the above analysis, the automated measurement method has demonstrated sufficient repeatability to operate on a distribution of cameras. For this study, a large number of uncooled cameras from the same manufacturing lot was considered. In this section, we show the camera-to-camera variations. The resolution, reported here as the MTF value at a certain spatial frequency, had the distribution seen in Figure 6. As can be seen, the distribution is asymmetric (fit to an extreme value probability density function), with the appearance of an upper bound. This can be understood as it is much more likely that there are aberrations or defocus between systems as opposed to manufacturing issues that would contribute to an improvement in performance (namely larger apertures). The max to min variation across the 250 systems was ~12%. The impact of this variation will depend on that specific task and whether it is blur or sensitivity dominated.

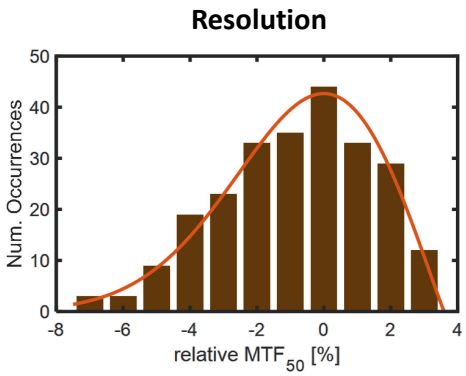


**Figure 6: Distribution of MTF values across 250 cameras.**

The distribution for noise (in units of mK) and time constant are shown in Figure 7. As can be seen, for this distribution of cameras, both the noise and the time constant appear to be bimodal, with unequal distributions to each mode. The distributions were fit to a double Gaussian model.

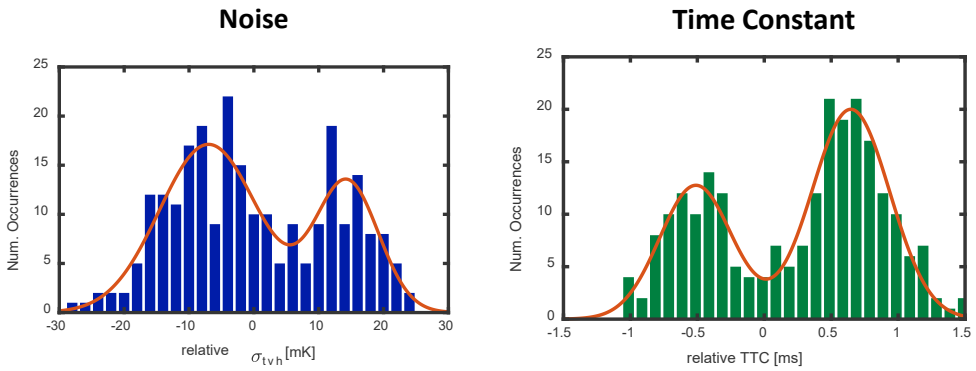


**Figure 7: (Left) The distribution of measured noise. (Right) The distribution of the time constant.**

Another useful metric to consider for the sensitivity is a combination of time constant and noise, known as the thermal camera figure of merit (FOM). It is typically assumed for a fixed detector geometry of an uncooled camera that multiplication of the time constant and tvh noise (in units of mK) is a constant.

$$FOM = \sigma_{tvh} \cdot \tau_{fit} \tag{3}$$

The FOM provides a convenient way to compare the sensitivity between different camera detectors. A plot of the FOM is shown below in Figure 8. The lines (and colors) correspond to a constant FOM, and the individual points are different cameras. In addition to the 250 cameras from the first program used above, measurements from other manufacturers and programs are also shown. As can be seen, the distributions for any particular program largely falls along a common trend.

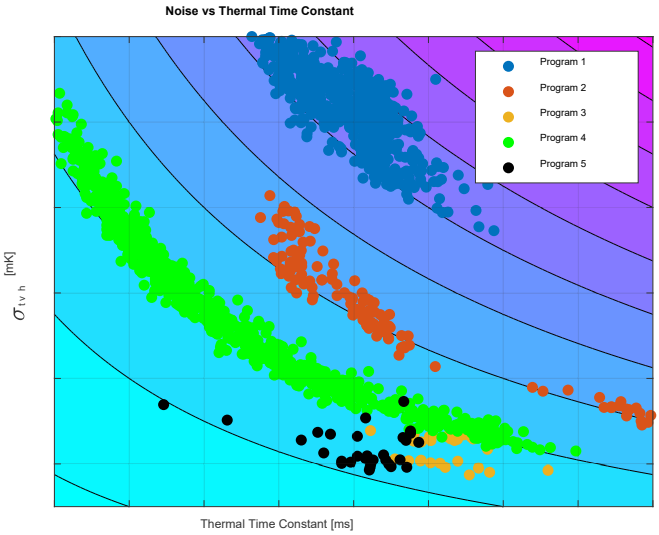


**Figure 8: A plot of the FOM for 5 different programs.**

The FOM is also a useful metric to evaluate if the sensitivity of the camera is changing in time. One common issue for an uncooled thermal camera is that it may lose vacuum pressure, leading to less efficient conversion of thermal energy into electrons. When this happens, both the conversion factor and time constant will reduce proportionally while the noise (in DN) remains the same. This means that the FOM will remain the same but the noise (in mK) increases as the time constant decreases. A demonstration of this phenomenon is shown below in Figure 9, where 20 cameras were measured periodically across a 60 month equivalent life cycle. The same color represents the same camera at it multiple measurements with time.

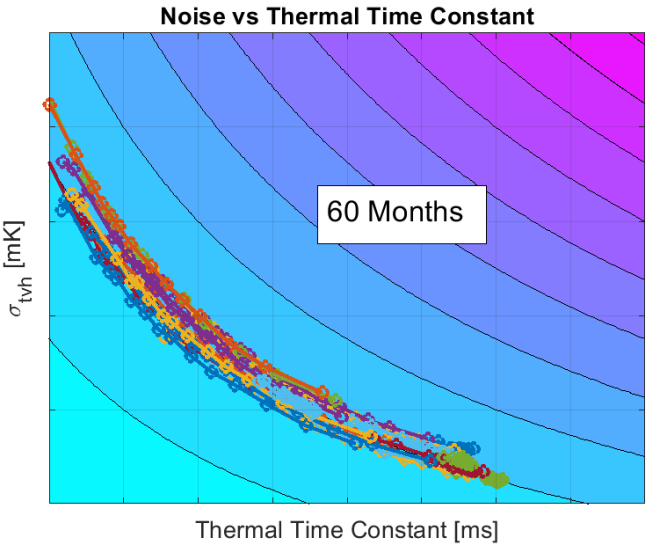


**Figure 9: A plot of the FOM for 20 cameras over time (same color is same camera).**

## 6.0 SUMMARY AND FUTURE DEVELOPMENT

In this correspondence, a rapid and automated method of evaluating thermal cameras was presented. The main developments consisted of automating device communication, automating capture and hardware interaction, utilizing individual blackbodies instead of a ramp (through the use of a rotation stage), automatic region of interest and post processing, and the implementation of parallel processing with capture. Automated methods such as these significantly reduced the reliance on the test engineer and potential for human errors. Through these methods, the time to completely characterize a thermal camera (including range performance and reporting and 2 SiTF runs) was reduced from 22.2 [min] down to 4.3 [min]. If only a single camera state measurement is required (i.e., no post processing noise), the total time for a full characterization is ~3.1 [min].

The automation allowed for a comprehensive repeatability study to be conducted, the results of which demonstrated that the automated methods are significantly more repeatable than any system-to-system variations. For example, the repeatability of the tvh noise was a standard deviation of 0.16 [mK] on a 73 [mK] average. When applied to a camera set of 250 uncooled cameras, manufacturing tolerances and device variations were able to be analyzed. This enabled the customer to ensure that all delivered cameras met specifications and to rank and order the cameras by performance. Additionally, the full measurement set allows for correlated statistics to be observed and model trades to be improved.

The methods and the repeatable results shown can serve as a baseline for evaluating other (less expensive) measurement solutions. Additional future developments and improvements on the setup will expand to larger

blackbodies to support larger aperture systems. Repeatability may also be improved with more care taken in controlling the ambient conditions. Creating a more generic mounting solution to facilitate the variety of systems is also something to consider in future generations. Finally, other measurements may be added, such as distortion and spectral response to meet the additional testing needs of the customers.

## 7.0 REFERENCES

[1] Haefner, D. P., https://www.mathworks.com/matlabcentral/profile/authors/4173815-david-haefner.

[2] Vollmerhausen, R. H., Jacobs, E. L., Hixson, J. G., and Friedman, M., "The targeting task performance (TTP) metric a new model for predicting target acquisition performance," tech. rep., Modeling and Simulation Division Night Vision and Electronic Sensors Directorate U.S. Army CERDEC Technical Report AMSEL-NV-TR-230(2006).

[3] Teaney, B., Reynolds, J. P., "Next generation imager performance model," Proc. SPIE 7662, 76620F (2010).

[4] Haefner, D. P., Burks, S., and Doe, J., "High throughput thermal camera characterization," Proc. SPIE 11740, 1174004 (2021).

[5] Teaney, B.P. and Haefner, D.P., "Evaluating the performance of an IR imaging system: a tutorial," Proc. SPIE 10625 (2016).

[6] Teaney, B.P., and Haefner, D.P., "Measured system component development for the night vision integrated performance model (NVIPM)", Proc. SPIE 9820 (2016).

[7] Burns, P. D., "Slanted-edge mtf for digital camera and scanner analysis," Proc. PICS Conf., IS&T, 135 (2000).

[8] Park, S. K. and Rahman, Z. "Fidelity analysis of sampled imaging systems," Optical Engineering 38 (5), (1999).

[9] Haefner. D. P., "Best Practices for Imaging System MTF Measurement," Electron. Imaging 2019 (10) (2019).

[10] Haefner, D.P., "MTF measurements, identifying bias, and estimating uncertainty", Proc. SPIE 10625 (2018).

[11] D'Agostino, J. A. and Webb, C. M., "Three-dimensional analysis framework and measurement methodology for imaging system noise," Proc. SPIE 1488 (1991).

[12] Haefner, D. P. and Burks, S. D., "Finite sampling corrected 3d noise with confidence intervals," Appl. Opt. 54, 4907 (4915) (May 2015).